The Influence of Strong Electron and Hole Doping on the Raman Intensity of Chemical Vapor-Deposition Graphene

Martin Kalbac,[†,§,*] Alfonso Reina-Cecco,[‡] Hootan Farhat,[‡] Jing Kong,[§] Ladislav Kavan,[†] and Mildred S. Dresselhaus[§,⊥]

[†]J. Heyrovský Institute of Physical Chemistry, Academy of Sciences of the Czech Republic, v.v.i., Dolejškova 3, CZ-18223 Prague 8, Czech Republic, [‡]Department of Materials Science and Engineering, MIT, Cambridge, Massachusetts 02139, United States, [§]Department of Electrical Engineering and Computer Science, MIT, Cambridge, Massachusetts 02139, United States, and [⊥]Department of Physics, MIT, Cambridge, Massachusetts 02139, United States

ABSTRACT Electrochemical charging has been applied to study the influence of doping on the intensity of the various Raman features observed in chemical vapor-deposition-grown graphene. Three different laser excitation energies have been used to probe the influence of the excitation energy on the behavior of both the G and G′ modes regarding their dependence on doping. The intensities of both the G and G′ modes exhibit a significant but different dependence on doping. While the intensity of the G′ band monotonically decreases with increasing magnitude of the electrode potential (positive or negative), for the G band a more complex behavior has been found. The striking feature is an increase of the Raman intensity of the G mode at a high value of the positive electrode potential. Furthermore, the observed increase of the Raman intensity of the G mode is found to be a function of laser excitation energy.

KEYWORDS: graphene · Raman spectroscopy · doping · electrochemical gating · spectroelectrochemistry

The unique properties of graphene are promising for many applications in nanoelectronics. The successful application of graphene requires a detailed understanding of its electronic properties, including both its neutral and doped states.

The doping of graphene leads to a shift of the Fermi level, and for this reason doping provides a simple way to control the transport and optical properties. In general, graphene can be doped chemically,[1] electrochemically,[2,3] or by electrostatic backgating[4−6] through a substrate. So far, most of the experiments have been performed using electrochemical or electrostatic doping because these methods provide an easy way to control the Fermi level of graphene. Electrostatic backgating is used because of its simplicity and its clear application link toward FETs, but there are several drawbacks to this approach. First, electrostatic doping is dependent on the properties of the dielectric. Since the doping efficiency is typically very low and a high voltage (up to 100 V) must be used, the available range of doping levels is limited. Also, a high applied voltage can change the properties of the substrate (due to charge trapping), making the results of the experiments more difficult to interpret. On the other hand, electrochemical doping is efficient, so that a voltage of ±1.5 V is usually sufficient for most doping experiments. The charge is mediated by an ohmic contact to the sample and compensated by an electrolyte counterion, which avoids problems with trapped charges. The response of graphene to electrochemical doping is also reasonably fast, and the speed of the measurement is usually limited only by the time take to acquire Raman signal in the spectrum. Nevertheless, the experiments are usually more difficult to carry out since the electrochemical setup brings specific requirements of the cell geometry, quality of the electrodes, purity of chemicals, *etc.* Also to achieve good control of the applied voltage, a three electrode system with a reference electrode must be used.[7]

Raman spectroscopy provides a convenient tool to characterize graphene since it can distinguish between monolayer, bilayer, and multilayer graphene, and Raman spectroscopy also is highly sensitive to the electronic structure of these materials.[8] The important features observed in the Raman spectra are the G mode and G′ mode (the latter also known as the 2D mode[9]). The G and G′ modes are present in all graphene-based materials; however, their frequencies, intensities, and line widths are influenced by other factors like the number of graphene layers, external doping, or laser excitation energy. In some graphene samples, the D line is also found and is believed to indicate the presence of defects as in ordinary graphite.

*Address correspondence to kalbac@jh-inst.cas.cz.

Received for review May 18, 2010 and accepted September 22, 2010.

Published online October 8, 2010.
10.1021/nn1010914

The graphene currently in use is usually obtained by the mechanical ("Scotch-tape") cleaving of individual atomic layers from graphite.[10] Other procedures are based on chemical exfoliation.[11] However, these methods lead to small graphene pieces (about 1−100 μm^2) randomly located on the substrate. This complicates the processing of such samples. The industrial use of these methods would be very difficult to develop and scale up. Recent advances in chemical vapor deposition (CVD) synthesis have now allowed the preparation of large and uniform monolayer graphene flakes.[12] The CVD prepared graphene thus significantly simplifies the materials processing, and more detailed studies with such samples can be readily performed, as discussed below.

Previous Raman studies made on mechanically cleaved graphene were focused on the evaluation of the frequency and line width, and the spectra of monolayer graphene were typically limited to one laser excitation wavelength (such as 514 nm).[2] It was found that electrochemical doping leads to a change of the width, frequency, and intensity of the Raman signal due to the removal of the Kohn anomaly.[2] However, the changes in signal intensity with electrode potential and the dependence of this intensity on laser excitation energy were discussed only partially in the literature, despite the significant effects that have been observed already.[2,3,13]

In the present paper we examine, for the first time, the Raman spectra of CVD-grown graphene as a function of doping level at three different laser excitations energies. The doping of graphene was realized using electrochemical charging. The PMMA/PC/$LiClO_4$ (PMMA = polymethylmethacrylate, PC = propylene carbonate) electrolyte has been used to ensure good performance of the electrochemical cell.[14] We focused on analyzing the change of the Raman intensity of the G and G′ bands as a function of the electrode potential. We observed for the first time an anomalous increase in the intensity of the G band at high positive electrode potentials with a significant dependence on the laser excitation energy. The G′ mode intensity decreased for both positive and negative values of the electrode potential similarly as in the case of experiments performed on cleaved graphene flakes.[2] This confirms that the electronic properties of graphene are not significantly dependent on the graphene preparation method.

RESULTS AND DISCUSSION

In our study we probed graphene synthesized by the CVD method when the graphene was transferred to a SiO_2/Si substrate and then embedded into a spectroelectrochemical cell. Figure 1A shows a typical Raman spectrum of such a CVD graphene sample on a SiO_2/Si substrate at an electrode potential $V_e = 0$ V, excited by 2.33 eV laser energy radiation. The spectrum is dominated by the two features typical for graphene-based materials: the G (TG) band at 1590 cm^{-1} and the G′ (2D) band at 2688 cm^{-1}. The D mode at about 1350 cm^{-1} indicates defects. The D/G ratio is about 0.28. The reason for the higher D/G ratio compared to that of cleaved graphene samples could be a smaller graphene domain size in the case of our CVD grown sample. Raman spectroscopy has been frequently used to distinguish a single layer of graphene (1-LG) from multilayer graphene (M-LG). It is generally accepted that the G′ band of M-LG is significantly broadened in comparison to the G′ band of 1-LG, and the relative intensities of the G band and G′ band change dramatically between 1-LG and M-LG. The fwhm line width of the G′ band in Figure 1A is about 30 cm^{-1}, which is typical for 1-LG. However, recently it has been shown that the broadening of the G′ band may be absent even in multilayer graphene, if the graphene sheets are misoriented relative to one another.[15] Another signature of 1-LG is the ratio between the G and the G′ mode intensities. This approach toward distinguishing between 1-LG and M-LG has been recently criticized[8] because the G′ mode intensity ($I_{G'}$) and the G mode intensity (I_G) are dependent on the doping level in a different way. Hence, if the doping state of the sample is unknown, the magnitude of the $I_{G'}/I_G$ ratio can be misleading. To avoid this problem related to doping, we show the Raman spectrum at a given electrode potential of 0 V (Figure 1A), which ensures that the effect of the natural doping (if any) is removed and the doping state of the graphene sample is controlled by the external applied potential only. A simple comparison of the G′ band and the G band peak heights in Figure 1A shows that the $I_{G'}/I_G$ is greater than 3. This confirms that our sample is indeed a single layer of graphene. Figure 1B shows an optical microscope image of the tested CVD sample. The darker part of the image corresponds to graphene while the brighter part of the image corresponds to the bare SiO_2/Si substrate. The thickness of a SiO_2 layer on top of Si was 300 nm, which is convenient for the determination of the number of graphene layers.[12] The presence of single layer graphene in our sample was confirmed by a color analysis as discussed recently.[12]

Figure 2 shows experimental spectra of CVD graphene at different electrode potentials for 2.33 eV laser excitation energy. The electrochemical charging is expected to change the frequency of both the G band (ω_G) and the G′ band ($\omega_{G'}$), which is in agreement with our observations. The Raman frequency of the G band is increased for positive potentials, and the maximum $\omega_G \approx 1618$ cm^{-1} was found at an electrode potential of 1.5 V, which was the largest electrode potential used in this experiment. For negative electrode potentials, ω_G increased until about a potential of −1.2 V and then again it is decreased slightly until −1.5 V. The maximum ω_G for negative potentials is 1604 cm^{-1} which is observed at a potential of about −1.2 V, while ω_G at an electrode potential of −1.5 V is 1602 cm^{-1}.

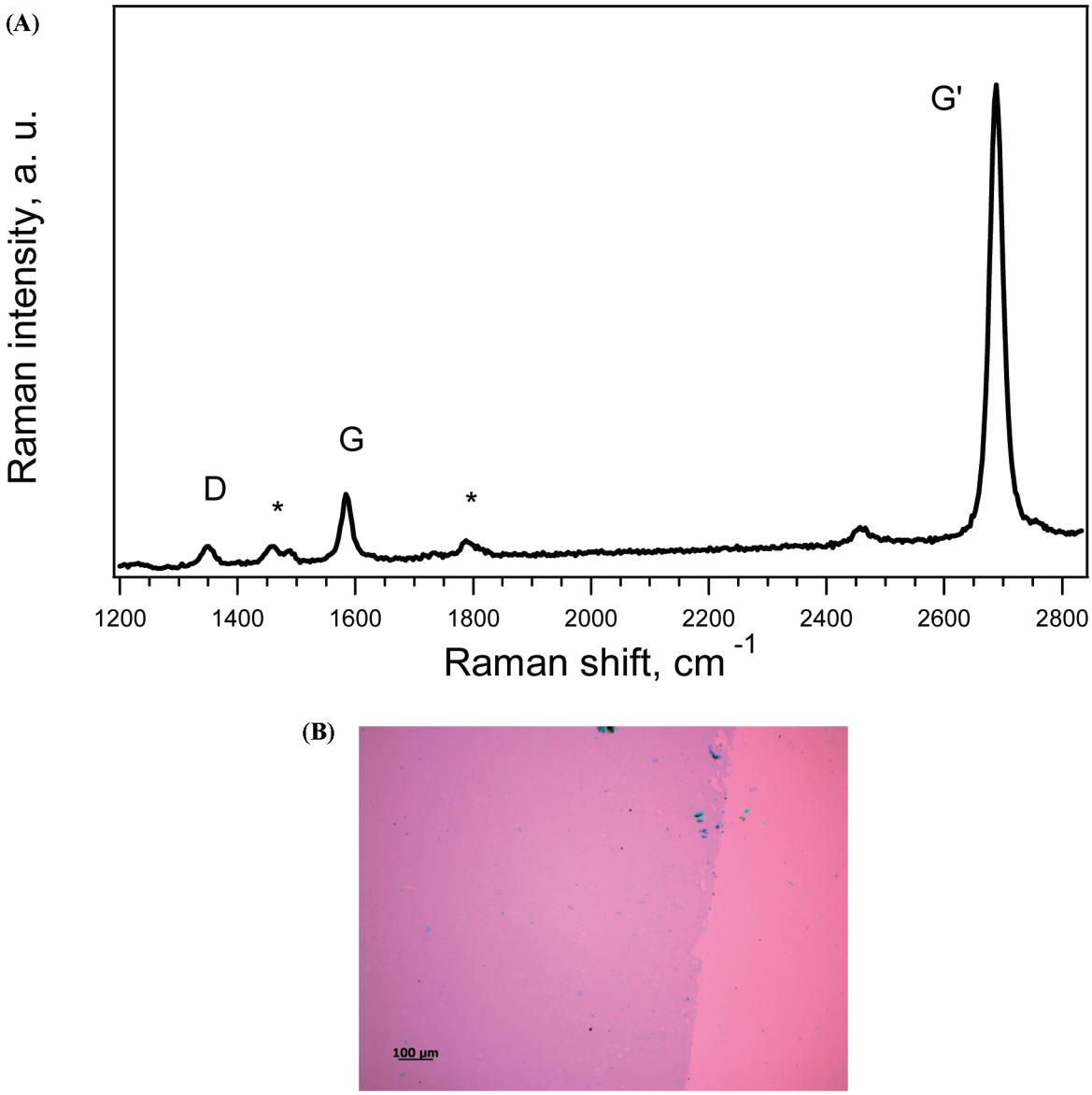

Figure 1. (A) Raman spectrum of single-layer CVD graphene at 0 V. The spectrum is excited by 2.33 eV (532 nm) laser excitation energy. Asterisks indicate Raman bands of the electrolyte. Figure 1B. Optical microscope image of the CVD graphene (darker area) sample on a SiO_2/Si substrate used for the Raman experiments reported in this paper.

The frequency shift of the G band in charged graphene is related to the change in the C−C bond strength and to the renormalization of the phonon energy.[16] In graphene a coupling between the lattice vibrations and Dirac fermions is allowed, because the scales for the electron and phonon dynamics are comparable. Therefore the adiabatic Born−Oppenheimer approximation fails to describe the G band phonons. Hence, time-dependent perturbation theory is used to explain the experimental observations. The carriers in graphene interact with phonons, and electron−hole pairs are created. This leads to a renormalization of both the phonon energy and the energy of the carriers. In charged graphene, the Fermi energy E_F is moved away from the Dirac point and thus the formation of electron−hole pairs is suppressed.[16] Due to electron−hole symmetry with respect to the Dirac point, the frequency shift of the G mode should be identical for both positive and negative doping. However, the doping also induces a change of the C−C bond strength.[6] The positive doping removes the electrons from antibonding orbitals, and therefore a hardening of the G band is expected. On the other hand, negative doping adds electrons to the antibonding orbitals which should lead to a softening of the Raman signal frequency (ω_G). Both phonon energy renormalization and a change of the bond strength occur, and the two effects are superimposed in the analysis of the experimental data. For positive doping both effects lead to an upshift of the phonon frequency. However, for negative doping they have an opposite effect on the frequency shift. This is consistent with the experimental results since a monotonic increase of the G band frequency was found at positive electrode potentials and

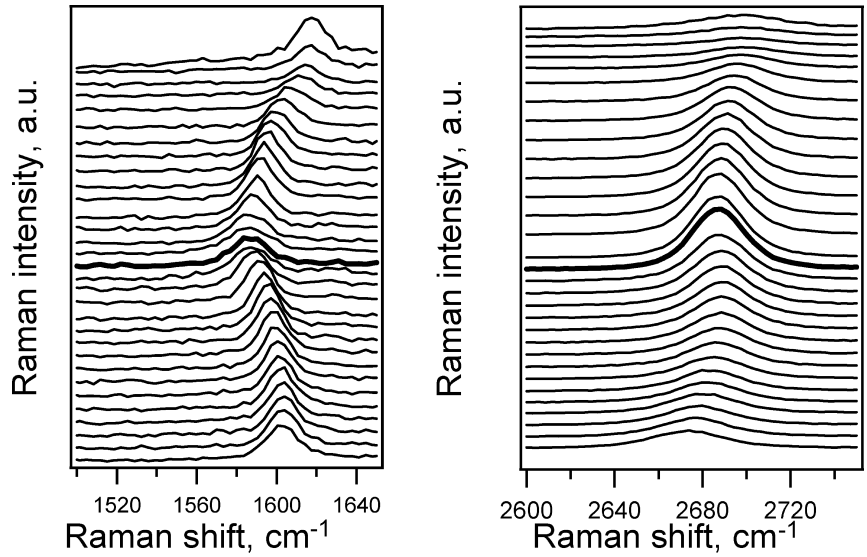

Figure 2. *In-situ* Raman spectroelectrochemical data for ω_G (left) and $\omega_{G'}$ (right) on graphene in the range from −1.5 to 1.5 V (from bottom to top). The spectra are excited by 2.33 eV (532 nm) laser radiation. The bold line traces denote the Raman spectrum ω_G and $\omega_{G'}$ at a potential of 0 V. The electrochemical potential change between adjacent curves in the Figure is 0.1 V. The spectra are offset for clarity, but the intensity scale is the same for all spectra.

a nonmonotonic change in frequency was observed for negative electrode potentials. Also, the observed shift never becomes as large for the negative potentials.

The dependence of ω_G on electrode potential has been previously analyzed for cleaved graphene flakes.[2] The results for the cleaved graphene flakes are similar to those for the CVD graphene studied here, which confirms the concept that the properties related to the electronic structure can be tuned independently of the graphene preparation procedure. We note that in previous studies different electrolytes and also different electrochemical setups have been used, and these differences explain some differences between the data that was obtained by different groups. In particular this is the case of the doping efficiency. Much larger electrode potentials had to be applied in previous works[2] to achieve the same effect as in the work presented here. For example, in the case of electron doping, we observed the maximum frequency shift $\omega_G = 1604$ cm^{-1} at a potential of about −1.2 V but it was necessary to apply a potential of about −4 V to reach the same shift of the G band as was observed in previous work.[2] (It should be noted that the potential of −4 V is below the decomposition potential of any possible electrolyte. This means that such measurements were not performed under equilibrium conditions and the potential at the graphene electrode was not properly controlled.) The better efficiency of our doping is important for an evaluation of the effects at higher doping levels since an electrolyte/electrode instability can occur at high electrode potentials. We attribute the better efficiency of our experiments to the different electrolyte rather than to a different procedure in the graphene preparation.

We also note that in our work we give the values of the potential of the working (graphene) electrode. Hence positive potentials correspond to hole doping and negative potentials to electron doping. This notation is intuitive and is commonly used in electrochemical works. On the other hand, in some other works, the potentials of the reference (gate) electrode are provided, which gives an opposite sign of the potential values; for example, in that work negative values of the electrode potential correspond to the hole doping of graphene, while positive potentials correspond to electron doping of the graphene.

The behavior of the G′ mode frequency $\omega_{G'}$ is also sensitive to the doping (Figure 2). We observe an increase in $\omega_{G'}$ with an increasing magnitude of the positive electrode potentials. On the other hand, for electron doping there is first an increase in $\omega_{G'}$, followed by a relatively large decrease in $\omega_{G'}$. The increase of $\omega_{G'}$ is weaker than in the case of ω_G for both positive and negative doping. For the potentials from 0 to 1 V, a slope of $\Delta\omega_{G'}/\Delta V = 9$ cm^{-1}/V was observed for the G′ mode, while the corresponding slope of the G mode was $\Delta\omega_G/\Delta V = 18$ cm^{-1}/V. The ratio of $\Delta\omega_G/\Delta V$ *vs* $\Delta\omega_{G'}/\Delta V$ is 2, which is in excellent agreement with theoretical prediction.[17] The maximum upshifted frequency at +1.5 V is about 2700 cm^{-1} compared to 2688 cm^{-1} at 0 V. For negative doping the maximum frequency is about 2690 cm^{-1}, but at −1.5 V, $\omega_{G'}$ is only 2675 cm^{-1} which is even below the value of $\omega_{G'}$ at 0 V (2688 cm^{-1}). The change Δ of $\omega_{G'}$ with respect to the electrode potential ($\Delta\omega_{G'}/\Delta V$) includes the effects of changes in the C−C bond strength, the electron−phonon coupling, and electron−electron interactions. Similarly, as in the case of ω_G, the hole doping increases $\omega_{G'}$ and electron doping decreases $\omega_{G'}$.

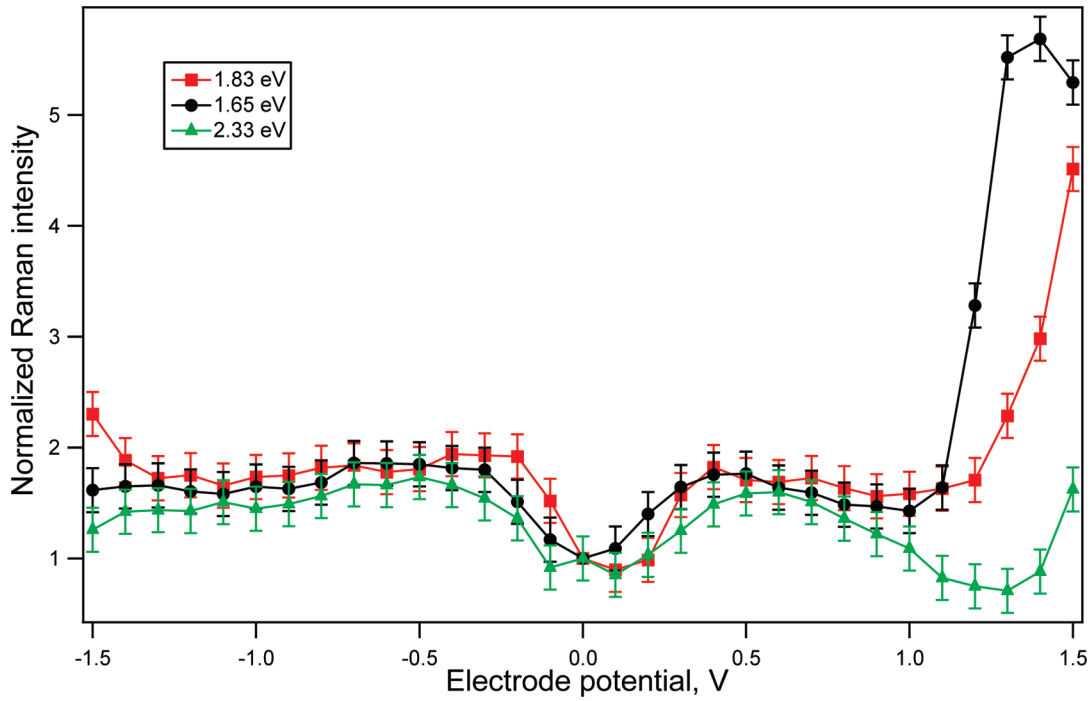

Figure 3. Raman intensity *vs* electrode potential profiles for the G mode. The intensities of the spectra at all electrode potentials are normalized to the intensity of the G mode at a potential of 0 V for each respective laser excitation energy. The spectra are excited by 2.33 eV (triangles), 1.83 eV (squares), and 1.65 eV (circles) laser excitation energies.

Raman Intensity. The Raman intensities of both the G and G′ modes for graphene (Figures 3 and 4) exhibit a significant dependence on electrode potential. However, the dependence of their intensities on the electrode potential is specific for each Raman mode. The signal intensity of the G′ band (see Figure 4) is monotonically decreased as the magnitude of the electrode potential is increased, both for positive and negative potential values. For the G band, we found a more complex behavior (see Figure 3), and this behavior is different for positive and negative values of the electrode potential. The interesting feature in the case of positive doping is a dramatic increase of the Raman G band intensity at high positive potentials which is not reproduced for negative doping. Nevertheless for positive potentials, the increase of the intensity is reproduced also for other laser excitation energies, as is shown later in this paper.

We first analyze the dependence of the Raman intensity of the G mode on electrode potential. In Figure 3 the intensity *vs* potential profile is plotted for the 2.33 eV laser excitation energy (data taken from Figure 2) and the results are shown in Figure 3 also for the 1.83 and 1.65 eV laser excitation energies.

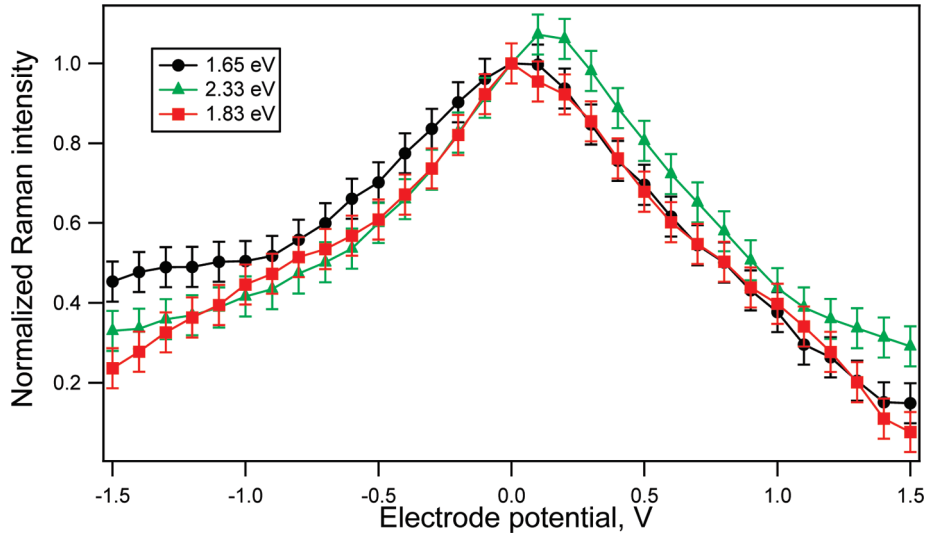

Figure 4. Raman intensity *vs* electrode potential profiles for the G′ mode. The spectra are excited by 2.33 eV (triangles), 1.83 eV (squares), and 1.65 eV (circles) laser excitation energy.

For all laser excitation energies, the intensity *vs* potential profiles in Figures 3 and 4 exhibit a similar complex shape. The profiles are not symmetrical for positive and negative doping. For negative doping there is a smaller increase in intensity in Figure 3 and then the intensity remains approximately constant up to a potential of −1.5 V. For positive doping a smaller increase of intensity was found at low potential values at the beginning of the doping process. For potentials with magnitudes between 0.5 and 1.0 V, the intensity remains approximately constant. Increasing the potential beyond +1 V leads to a slight decrease of the intensity which is followed by a strong increase of the intensity for higher voltages. No significant intensity decrease in Raman intensity is found for 1.83 and 1.65 eV laser excitation energies. The final increase of intensity above 1.0 V depends on the laser excitation energy and it is found to be stronger for lower laser excitation energies. For the 2.33 eV laser excitation energy, the Raman intensity of the G mode at an electrode potential 1.5 V is about 1.5 times higher than at the potential of 0 V. For lower laser excitation energies the anodic enhancement of the signal is even more pronounced. For $E_{laser} = 1.83$ eV, the Raman intensity at 1.5 V is about 4 times higher, and for $E_{laser} = 1.65$ eV it is even higher (7 times). This complex behavior is not reproduced for negative electrode potentials. We note that a slight increase of the Raman intensity may be traced also in the case of the doping of graphene studied previously using the 2.41 eV laser excitation energy.[2] However, due the lower efficiency of the doping, this effect appeared at very high electrode potentials, where also a degradation of the electrolyte and other effects may occur. Also this effect in Figure 3 is the weakest for the 2.33 eV laser excitation energy, which is close to the 2.41 eV used in the previous study,[2] and therefore the dramatic increases shown in Figure 3 were not observed previously.

The bleaching of the intensity of the Raman signal by varying the doping level has been observed also for SWCNTs (both metallic and semiconducting).[18,19] In the case of SWCNTs, the bleaching of the Raman signal was explained by the filling of the Van Hove singularities which are in resonance with the laser excitation energy.[18,19] However, recently this simple model has been revised and it was suggested that the Raman signal reflects a change in the electronic structure of single wall carbon nanotubes, which occurs in the case of the filling of any electronic state. The filling of the Van Hove singularity which is in resonance with the laser excitation energy is therefore not a prerequisite for the bleaching of the Raman signal.[18] Nevertheless, the experiments which probed different electronic transitions of the same tube showed that if the filled Van Hove singularities are in resonance with the laser excitation energy, then the bleaching effect is stronger than in the case where the electronic states, which are not in resonance with the laser excitation energy, are either filled or depleted.[20]

For graphene no singularities are present in the electronic structure (except for narrow graphene nanoribbons), which excludes a resonance effect at particular values of the laser energy radiation. Nevertheless, the filling of the electronic states should also be reflected by a change in the Raman spectra.

The G-band intensity drop at 0 V in Figure 3 is obviously related to the broadening of the G band.[21] In undoped samples the phonons can dissipate energy by forming an electron−hole pair.[16,21] In doped samples this process is suppressed because the final state is occupied (for electron doping) or it is empty (for p doping) and therefore the G band is narrowed.[6,16,21] After the Kohn anomaly effect is removed, the G band intensity is not changed by further negative doping and up to 1.0 V for positive doping, which is consistent with previous theoretical predictions and experimental results.[6] At positive potentials above 1.0 V we observed an anomalous increase of the G mode intensity for $E_{laser} = 1.65$ eV. A strong increase in the G band intensity also occurred above 1.2 V potential for $E_{laser} = 1.83$ eV. The enhancement of the Raman signal at high positive potentials is counterintuitive; nevertheless, it is consistent with recent theoretical work by Basko.[22] His calculation suggests that the matrix element for the G band increases when the Fermi level is close to the $E_{laser}/2$. It is also obvious that if the laser excitation energy decreases then the Fermi level will reach $E_{laser}/2$ at lower magnitudes of electrode potentials. The anodic enhancement of the G mode intensity observed in Figure 3 is obviously a consequence of the latter situation, and this is in agreement with our observation that the strongest enhancement is found for the 1.65 eV laser excitation energy and the overall effect is weakest for the 2.33 eV laser excitation energy. In other words, the highest energy laser excitation (2.33 eV) shows only an onset of the enhancement effect in the +1.0 to +1.5 V potential range. It might be expected that at even higher electrode potentials we would observe the same enhancement effect as is seen at $E_{laser} = 1.65$ eV. Unfortunately, higher potentials were not accessible in the present work due to limited electrolyte stability.

Figure 4 shows the dependence of the Raman intensity of the G′ mode on electrode potential for $E_{laser} = 2.33$ eV (data taken from Figure 2) and for two additional laser excitation energies (1.83 and 1.65 eV). In contrast to the intensity *vs* potential profiles observed for the G band, here for the G′ band we found a monotonic decrease of the intensity for both positive and negative doping. Note that the slope of the intensity decrease of the G′ mode is smaller for negative doping than for positive doping. The intensity of the G′ mode at −1.5 V is about 5 times weaker than at 0 V, and for +1.5 V, it is about 7 times weaker. There is a

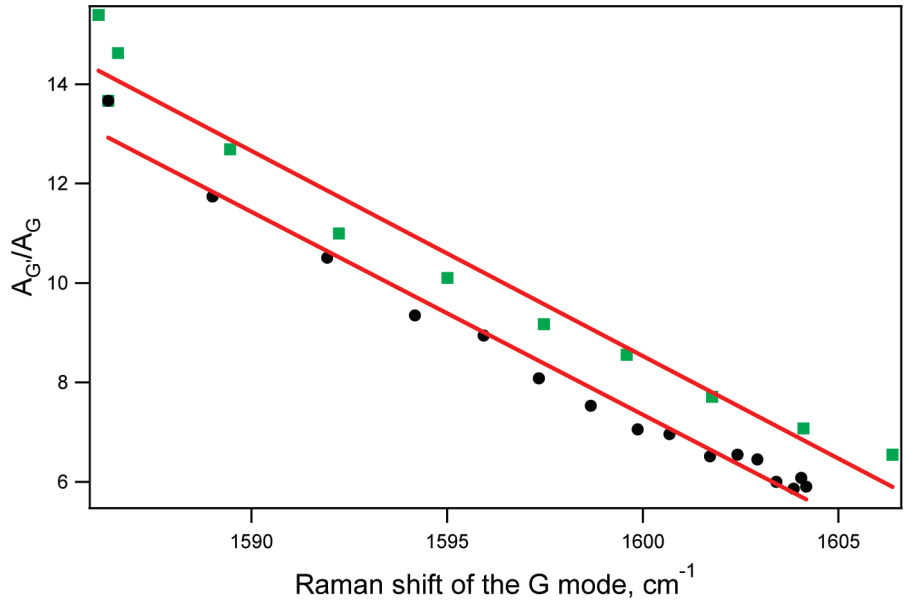

Figure 5. A plot of the A_G'/A_G ratios *vs* Raman frequency of the G mode ω_G. Squares correspond to positive doping, and circles correspond to the negative doping. The straight lines correspond to the fits of the data by the linear relations: $A_G'/A_G = a - b\omega_G$, where $a = 669$, $b = 0.413$ for positive doping and $a = 660$, $b = 0.408$ for negative doping.

variation of the bleaching for different laser excitation energies but this dependence on E_{laser} is relatively small.

It has been suggested previously[3] that the intensity of the G′ band ($I_{G'}$) is proportional to the electron/hole inelastic scattering rate. Doping will increase the number of charge carriers and therefore the probability of a scattering event will also increase and the G′ band intensity should therefore decrease.[3]

The asymmetry of the decrease $I_{G'}$ with respect to the electron and hole doping is analogous to that observed for SWCNTs. In the latter case, the asymmetry is consistent with the general fact that the density of states for the π^* band is smaller (energy bandwidth is larger) than that for the π band. In other words, for the π^* band, E_F must be moved more to inject a given amount of carriers than for the π band. However, the band structure of graphene is expected to be symmetric with respect to the Dirac point, hence no asymmetry should be observed. Nevertheless, the following facts must be also considered: (1) Graphene is usually p-doped from the substrate.[23] The p-doping can partly compensate the charge injected during negative doping, hence the effect of negative doping is less pronounced compared to the positive doping. (2) The asymmetry may also come from the relaxation time of photoexcited carriers. In the case of negative doping, electrons occupy the π^* band. Thus the relaxation of the photoexcited carrier becomes slow. In the case of hole doping, the states below the Dirac point are empty and the relaxation is fast. This asymmetry should be larger for a lower excitation energy of the laser since the photoexcited carriers are generated close to the Dirac point. Indeed the lowest excitation energy (1.65 eV) exhibits the strongest asymmetry experimentally.

Since the time of the early studies on graphene, the large magnitude of the A_G'/A_G ratio (A denotes integrated area of the peak) has been used as an indicator of single layer graphene. Up to this point in the paper we used peak heights of the Raman bands for characterizing the Raman intensities since it is a more straightforward approach and we could also easily demonstrate the effect of the Kohn anomaly in this way (Figure 3). However, for the identification of 1-LG the integrated peak area of the G and the G′ features is more convenient since it is not affected by the Kohn anomaly (a change of the G band height is compensated by a change of the G bandwidth). The integrated area of the G′ mode is a function of doping. The frequency of the G band ω_G is also a function of the doping and therefore ω_G could be used as an indicator of doping level and thus for correction of the A_G'/A_G ratio as a function of the amount of doping. Figure 5 shows a plot of the A_G'/A_G ratio *vs* ω_G from the data obtained using the 2.33 eV laser excitation energy, which is the widely used E_{laser} energy. The data for both negative and positive electrode potentials are included in Figure 4. Nevertheless we fit them separately, since the A_G'/A_G ratio exhibits a slightly different behavior for positive and negative doping. For positive doping we also excluded data for potentials from 1.1 to 1.5 V due to the anomalous behavior of the G mode. The linear fits of the dependence give the following relation:

$$A_G'/A_G = a - b\omega_G \qquad (\text{for } \omega_G \text{ in } cm^{-1}) \qquad (1)$$

where $a = 669$, $b = 0.413$ for positive doping and $a = 660$, $b = 0.408$ for negative doping.

It is clear from Figure 5 that the development of the A_G'/A_G ratio as a function of ω_G is reproduced very

well by eq 1, which may serve to correct the A_G'/A_G ratio associated with doping and allow for an easy identification of single layer graphene. The A_G'/A_G ratio as a function of ω_G exhibits a slight difference between positive and negative doping which is due to an asymmetry in the bleaching of the G′ mode with respect to positive and negative doping as discussed earlier in this study.

CONCLUSION

We studied the dependence of the graphene Raman features (the G and G′ modes) on the electrode potential for CVD grown single-layer graphene. The dependence of ω_G and $\omega_{G'}$ on the electrode potential for CVD grown graphene is similar to that reported for cleaved graphene flakes. However, our experimental setup provides better doping efficiency than in the case of previous works, so that parasitic effects like electrolyte decomposition or nonequilibrium states at high electrode potential could be avoided.

We also found a strong difference in the electrode potential dependence of I_G relative to that of $I_{G'}$. The G mode exhibited an asymmetry in the electron/hole doping with a striking increase in intensity observed only for hole doping, and this effect was not recognized in previous experimental works. On the other hand, the G′ mode showed a decrease in intensity both for electron and hole doping. The detailed understanding of the effects of doping is important not only for fundamental reasons but also for practical experiments. The intensity ratio A_G'/A_G at zero potential is one of the experimental parameters which could be used to distinguish between one and two graphene layers. But the present work shows that the A_G'/A_G ratio is strongly dependent on the doping level. Here we related the change in the A_G'/A_G ratio due to doping to the change of ω_G with doping. The latter relation could be fitted by a simple linear equation, which can then be used to correct the A_G'/A_G ratio of doped samples to approximate its corresponding value for a neutral sample.

EXPERIMENTAL SECTION

Graphene samples were synthesized using the CVD method.[12] The details are provided in previous work.[12] In brief: A Ni film deposited on a SiO_2/Si substrate is heated to 900 °C and annealed for 20 min under flowing H_2 and Ar gas (400 and 600 sccm (standard cubic centimeter per minute), respectively). Then the film was exposed to H_2 and CH_4 for 5 min, and finally the substrate was cooled down from 1000 to 500 °C under Ar, H_2, and CH_4. The as-grown graphene was subsequently transferred to a clean SiO_2/Si substrate using PMMA, according to procedures reported previously.[12]

For the doping experiments, graphene samples on a SiO_2/Si substrate served as working electrodes, and the samples were contacted using Au evaporated on a part of the substrate. The cell was completed with a Pt-counter electrode and an Ag-wire pseudoreference electrode. The electrolyte solution used was 0.1 M $LiClO_4$ dissolved in dry propylenecarbonate/PMMA (Aldrich). Electrochemical doping of the working graphene electrode was carried out by varying the applied potential between −1.5 and 1.5 V *vs* an Ag pseudoreference electrode (PAR potentiostat). We used a three electrode system and carried out measurements in the potentiostatic regime, so that no current was flowing through the reference electrode during the measurements, and care was also taken that the current flow through the working electrode was minimal. As the state (potential) of the pseudoreference electrode is not changed during the measurement, the applied potential on the working electrode is well-defined. The Raman spectra were excited by a Kr^+ laser (Coherent), a Ti-sapphire laser (Coherent), or a Nd:YAG laser (Coherent). The spectrometer resolution was about 5 cm^{-1}. The spectrometer was interfaced to a microscope (Carl-Zeiss, objective 100×). The size of the laser spot was about 0.5 μm. The peak intensities (I) correspond to the peak amplitudes of the Lorentzian fit of the analyzed Raman spectra. The error was estimated as a maximum deviation between two experimental points in two independent measurements multiplied by a factor of 2.

Acknowledgment. This work was supported by the Academy of Sciences of the Czech Republic (contract No. IAA400400911, IAA400400804, and KAN200100801), Czech Ministry of Education, Youth and Sports (ME09060 and LC-510), and Czech Grant agency (203/07/J067, P204/10/1677). The work done at MIT was supported by NFS-DMR 07-04197. The authors are grateful to Prof. R. Saito and Dr. D. Basko for helpful discussions.

REFERENCES AND NOTES

1. Jung, N.; Kim, N.; Jockusch, S.; Turro, N. J.; Kim, P.; Brus, L. Charge Transfer Chemical Doping of Few Layer Graphenes: Charge Distribution and Band Gap Formation. *Nano Lett.* **2009**, *9*, 4133–4137.
2. Das, A.; Pisana, S.; Chakraborty, B.; Piscanec, S.; Saha, S. K.; Waghmare, U. V.; Novoselov, K. S.; Krishnamurthy, H. R.; Geim, A. K.; Ferrari, A. C.; Sood, A. K. Monitoring Dopants by Raman Scattering in an Electrochemically Top-Gated Graphene Transistor. *Nat. Nanotechnol.* **2008**, *3*, 210–215.
3. Basko, D. M.; Piscanec, S.; Ferrari, A. C. Electron−Electron Interactions and Doping Dependence of the Two-Phonon Raman Intensity in Graphene. *Phys. Rev. B* **2009**, *80*, 165413.
4. Freitag, M.; Steiner, M.; Martin, Y.; Perebeinos, V.; Chen, Z. H.; Tsang, J. C.; Avouris, P. Energy Dissipation in Graphene Field-Effect Transistors. *Nano Lett.* **2009**, *9*, 1883–1888.
5. Malard, L. M.; Pimenta, M. A.; Dresselhaus, G.; Dresselhaus, M. S. Raman Spectroscopy in Graphene. *Phys. Rep.* **2009**, *473*, 51–87.
6. Yan, J.; Zhang, Y. B.; Kim, P.; Pinczuk, A. Electric Field Effect Tuning of Electron−Phonon Coupling in Graphene. *Phys. Rev. Lett.* **2007**, *98*, 166802.
7. Kavan, L.; Kalbac, M.; Zukalova, M.; Dunsch, L. Comment on "Determination of the Exciton Binding Energy in Single-Walled Carbon Nanotubes. *Phys. Rev. Lett.* **2007**, *98*, 019701.
8. Ferrari, A. C.; Meyer, J. C.; Scardaci, V.; Casiraghi, C.; Lazzeri, M.; Mauri, F.; Piscanec, S.; Jiang, D.; Novoselov, K. S.; Roth, S.; Geim, A. K. Raman Spectrum of Graphene and Graphene Layers. *Phys. Rev. Lett.* **2006**, *97*, 187401.
9. Thomsen, C.; Reich, S. Double Resonant Raman Scattering in Graphite. *Phys. Rev. Lett.* **2000**, *85*, 5214–5217.
10. Novoselov, K. S.; Geim, A. K.; Morozov, S. V.; Jiang, D.; Katsnelson, M. I.; Grigorieva, I. V.; Dubonos, S. V.; Firsov, A. A. Two-Dimensional Gas of Massless Dirac Fermions in Graphene. *Nature* **2005**, *438*, 197–200.
11. Hernandez, Y.; Nicolosi, V.; Lotya, M.; Blighe, F. M.; Sun, Z. Y.; De, S.; McGovern, I. T.; Holland, B.; Byrne, M.; Gun'ko, Y.; *et al.* High-Yield Production of Graphene by Liquid-Phase Exfoliation of Graphite. *Nat. Nanotechnol.* **2008**, *3*, 563–568.
12. Reina, A.; Jia, X. T.; Ho, J.; Nezich, D.; Son, H. B.; Bulovic, V.;

Dresselhaus, M. S.; Kong, J. Large Area, Few-Layer Graphene Films on Arbitrary Substrates by Chemical Vapor Deposition. *Nano Lett.* **2009**, *9*, 30–35.
13. Das, A.; Chakraborty, B.; Piscanec, S.; Pisana, S.; Sood, A. K.; Ferrari, A. C. Phonon Renormalization in Doped Bilayer Graphene. *Phys. Rev. B* **2009**, *79*, 155417.
14. Kalbac, M.; Kavan, L.; Dunsch, L. *In Situ* Raman Spectroelectrochemistry of SWCNT Bundles: Development of the Tangential Mode During Electrochemical Charging in Different Electrolyte Solutions. *Diamond Relat. Mater.* **2009**, *18*, 972–974.
15. Poncharal, P.; Ayari, A.; Michel, T.; Sauvajol, J. L. Raman Spectra of Misoriented Bilayer Graphene. *Phys. Rev. B* **2008**, *78*, 113407.
16. Lazzeri, M.; Mauri, F. Nonadiabatic Kohn Anomaly in a Doped Graphene Monolayer. *Phys. Rev. Lett.* **2006**, *97*, 266407.
17. Piscanec, S.; Lazzeri, M.; Mauri, F.; Ferrari, A. C.; Robertson, J. Kohn Anomalies and Electron−Phonon Interactions in Graphite. *Phys. Rev. Lett.* **2004**, *93*, 185503.
18. Kalbac, M; Farhat, H.; Kavan, L.; Kong, J.; Sasaki, K.; Saito, R.; Dresselhaus, M. S. Electrochemical Charging of Individual Single-Walled Carbon Nanotubes. *ACS Nano* **2009**, *3*, 2320–2328.
19. Kalbac, M.; Kavan, L.; Dunsch, L. Changes in the Electronic States of Single Walled Carbon Nanotubes as Followed by a Raman Spectroelectrochemical Analysis of the Radial Breathing Mode. *J. Phys. Chem. C* **2008**, *112*, 16759–16763.
20. Kalbac, M; Kavan, L. The Influence of the Resonant Electronic Transition on the Intensity of the Raman Radial Breathing Mode of Single Walled Carbon Nanotubes During Electrochemical Charging. *J. Phys. Chem. C* **2009**, *113*, 16408–16413.
21. Piscanec, S.; Lazzeri, M.; Robertson, J.; Ferrari, A. C.; Mauri, F. Optical Phonons in Carbon Nanotubes: Kohn Anomalies, Peierls Distortions, and Dynamic Effects. *Phys. Rev. B* **2007**, *75*, 035427.
22. Basko, D. M. Calculation of the Raman G Peak Intensity in Monolayer Graphene: Role of Ward Identities. *New. J. Phys.* **2009**, *11*, 095011.
23. Casiraghi, C. Probing Disorder and Charged Impurities in Graphene by Raman Spectroscopy. *Phys. Status Solidi R* **2009**, *3*, 175–177.